Journal of Alloys and Compounds 509 (2011) 5070–5074

Contents lists available at ScienceDirect

Journal of Alloys and Compounds

journal homepage: www.elsevier.com/locate/jallcom

Ferroelectric relaxor behavior and dielectric spectroscopic study of $0.99(Bi_{0.5}Na_{0.5}TiO_3)$–$0.01(SrNb_2O_6)$ solid solution

K.N. Singh*, P.K. Bajpai

Advance Material Research Laboratory, Department of Pure & Applied Physics, Guru Ghasidas Vishwavidyalaya, Bilaspur 495009, India

ARTICLE INFO

Article history:
Received 2 September 2010
Received in revised form
24 December 2010
Accepted 29 December 2010
Available online 4 January 2011

Keywords:
X-ray diffraction
Ferroelectrics
Crystal structure
Dielectric response

ABSTRACT

$0.99(Bi_{0.5}Na_{0.5}TiO_3)$–$0.01(SrNb_2O_6)$ was prepared by simple solid state reaction route. Material stabilized in rhombohedral perovskite phase with lattice constants $a = 3.9060$ Å, $\alpha = 89.86^\circ$ and $a_h = 5.4852$ Å, $c_h = 6.7335$ Å for hexagonal unit cells. Density of material was found 5.52 g_m/cm^3 (92.9% of theoretical one) in the sample sintered at 950 °C. The temperature dependent dielectric constant exhibits a broad peak at 538 K ($\varepsilon_m = 2270$) at 1 kHz that shows frequency dependent shifts toward higher temperature – typical relaxor behavior. Modified Curie–Weiss law was used to fit the dielectric data that exhibits almost complete diffuse phase transition characteristics. The dielectric relaxation obeys the Vogel–Fulcher relationship with the freezing temperature 412.4 K. Significant dielectric dispersion is observed in low frequency regime in both components of dielectric response and a small dielectric relaxation peak is observed. Cole–Cole plots indicate polydispersive nature of the dielectric relaxation; the relaxation distribution increases with increase in temperature.

1. Introduction

Relaxor ferroelectrics have drawn attention due to their applications in various microelectronics devices. Most of relaxor materials such as $Pb(Mg_{1/3}Nb_{2/3})O_3$, $Pb(Sc_{1/3}Nb_{2/3})O_3$ and their derived compounds [1,2] are used as high capacitance capacitor, hysteresis free actuators and high performance sensors. However, due to volatility and toxicity of lead, attempts have been made to develop lead-free compositions for environmental friendly applications. A number of lead free materials are designed and characterized as ferroelectric relaxors. However, all the materials are either complicated to synthesize or less promising in their physical properties than current Pb-based systems. Therefore, need for developing better lead free systems with enhance physical and electrical characteristics. Bismuth sodium titanate, $Bi_{0.5}Na_{0.5}TiO_3$ (BNT), discovered by Smolenski et al. [3] is one of the important ferroelectrics with perovskite structure. But Bi ion is highly volatile at high temperature above 1130 °C during sintering and making this material difficult to pole due to its high conductivity [4]. Although, most investigations have been concentrated on the modifications of BNT for applications such as piezoelectric and pyroelectric devices, this material is considered to be good candidate for a high temperature relaxor. Recently, some investigations have been done on the search for the modifications in the BNT-based systems [5,6]. To improve the piezoelectric properties, a number of BNT-based solid solutions, such as BNT–$Bi_{0.5}K_{0.5}TiO_3$ [7], $(1-x-y)Bi_{0.5}Na_{0.5}TiO_3$–$xBi_{0.5}K_{0.5}TiO_3$–$yBi_{0.5}Li_{0.5}TiO_3$ [8], BNT–$NaNbO_3$ [9], BNT–$BaTiO_3$–$Bi_{0.5}Li_{0.5}TiO_3$ [10], $Bi_{0.5}Na_{0.5}TiO_3$–$SrTiO_3$–$Bi_{0.5}Li_{0.5}TiO_3$ [11], BNT–$Bi_{0.5}K_{0.5}TiO_3$–$BaTiO_3$ [12] and $Bi_{0.5}Na_{0.5}TiO_3$–$Bi_{0.5}Li_{0.5}TiO_3$ [13] have been developed and studied intensively [14]. The $Bi_{0.5}Na_{0.5}TiO_3$-based piezoelectric substituted by Ba^{2+} [15,16] and the effect of Ba^{2+} in BNT ceramics on dielectric and conductivity properties have been studied [17]. Piezoelectric and dielectric properties of $(1-x)$BNT–xBT (abbreviated as BNBT) ceramics were improved by using additives as CeO_2 [18], Ga_2O_3 [19], Y_2O_3 [20], La_2O_3 [21], $YMnO_3$ [22] and $BaTiO_3$-doped $(Bi_{0.5}Na_{0.5})TiO_3$ [23]. However, the piezoelectric properties of these ceramics are not enough for practical uses. In order to further enhance the properties of BNT ceramics and meet the requirements for practical uses, it is necessary to develop new BNT-based ceramics.

BNT based lead-free ceramic materials $(1-x)$ $Bi_{0.5}Na_{0.5}TiO_3$–$xBaNb_2O_6$, exhibited relaxor characteristic different from classic relaxor ferroelectrics. Moreover, it can also be found that the samples of BNT–BN having lower concentration of BN ($x = 0.002$ and 0.006) shows completely different dielectric relaxor characteristic from higher concentration of BN ($x = 0.01$ and 0.14) [24]. It motivated us to synthesize another non-lead based perovskite in single phase with 1% doping level of $SrNb_2O_6$ (SN) in ferroelectric phase of BNT ceramic with relatively low sintering temperature. In this paper we investigate the ferroelectric relaxor behavior dielectric relaxation in $0.99(Bi_{0.5}Na_{0.5}TiO_3)$–$0.01(SrNb_2O_6)$ abbreviated as BNT–SN by means of dielectric spectroscopy.

* Corresponding author. Tel.: +91 7752 260249; fax: +91 7752 260148.
E-mail address: knsingh.ggv@gmail.com (K.N. Singh).

0925-8388/$ – see front matter © 2011 Elsevier B.V. All rights reserved.
doi:10.1016/j.jallcom.2010.12.195

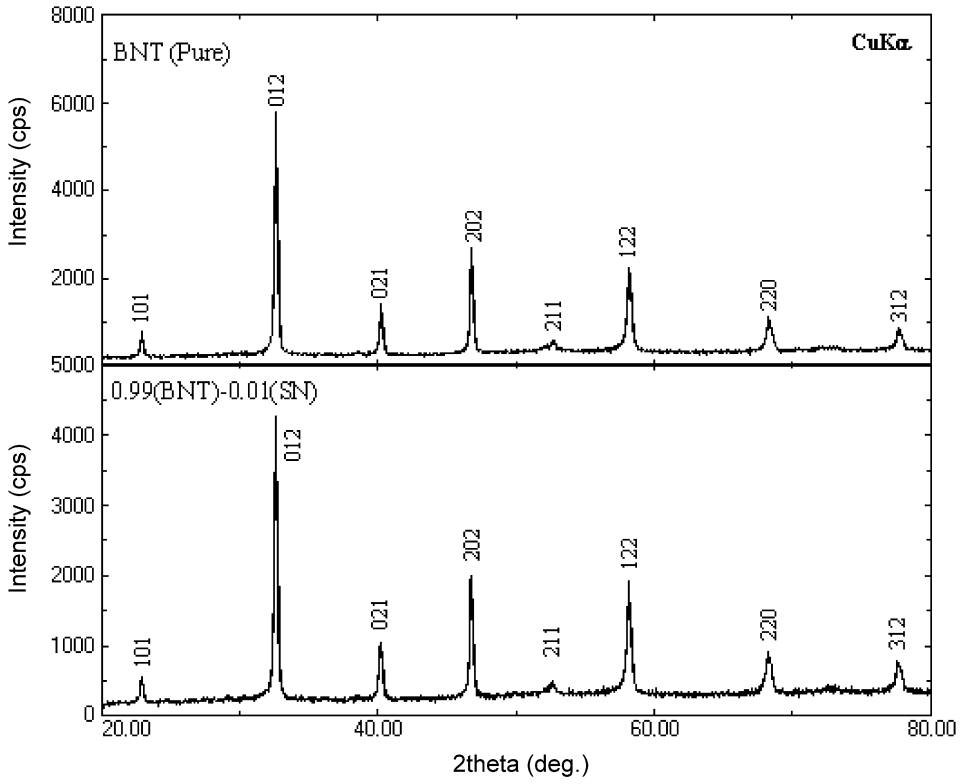

Fig. 1. XRD profile of calcined powder of pure BNT and BNT–SN at room temperature.

2. Experimental

A conventional ceramic fabrication technique was adopted to prepare $0.99(Bi_{0.5}Na_{0.5}TiO_3)$–$0.01(SrNb_2O_6)$ ceramic. GR grade oxide and carbonate powders Bi_2O_3, TiO_2, Nb_2O_5, $SrCO_3$ and Na_2CO_3 were used as starting materials. The stoichiometric amounts of constituent's powders were mixed in wet medium (acetone) for 5 h. The mixed powder were calcined at 900 °C for 3 h at the rate of 2 °C/m. Calcined powder were structurally analyzed using X-ray diffraction data which were carried out using X-ray diffractometer (Rigaku, Miniflex) with Cu K_α $\lambda = 1.54056$ Å. Fine calcined powder were pressed into cylindrical pellets of 10 mm diameter and 1–2 mm thickness under an isostatic pressure of 100 MPa. Polyvinyl alcohol (PVA) was used as a binder. The pellet were sintered at 950 °C for 3 h and cooled down to room temperature using controlled cooling rate 2 °C/m. To determine the dielectric properties, the sintered sample were electroded with silver paste and heated at 500 °C for 2 h before measurements were performed. The electrical measurements were performed at various temperatures, using a computer controlled LCR HI-TESTER (HIOKI-3532-50) impedance analyzer.

3. Results and discussion

3.1. X-ray diffraction study

Fig. 1 shows the X-ray diffraction patterns of pure BNT and BNT–SN in the 2θ range of 20–80°. All the reflection peaks of the X-ray profile were indexed and lattice parameters were determined using a least-squares method with the help of a standard computer programme (POWD) [25]. It can be seen from Fig. 1, the prepared system shows rhombohedral perovskite phase. The lattice constants obtained for perovskite phase of BNT–SN is $a = 3.9060$ Å, $\alpha = 89.86°$ for rhombohedral and $a_h = 5.4852$ Å, $c_h = 6.7335$ Å for hexagonal unit cells. The estimated lattice parameters are matched well with earlier reports [26,27] (JCPDF No-36-0340). From XRD analysis, it is evident that $SrNb_2O_6$ diffused into BNT lattice and does not cause any observable phase change in the structure. However, with the inclusion of Sr at A-site and Nb at B-site, expands the unit cell. Density of material was found 5.52 g_m/cm^3 (92.9% of theoretical one) in the sample sintered at 950 °C.

3.2. Dielectric study

Pure BNT, shows two abnormal dielectric peaks which originate from phase transition from ferroelectric to anti-ferroelectric (at T_f) and anti-ferroelectric to paraelectric phase (at T_m) [26–28]. In BNT–SN system both peaks get merged may be due to inclusion of Sr^{2+} at A-site and Nb^{5+} at B-site. The dielectric characterization of relaxors has mainly focused on investigating the temperature dependence above T_m used for characterizing the degree of dielectric relaxation [29–31]. The temperature dependence of dielectric constants for BNT–SN at different frequencies is shown in Fig. 2. The

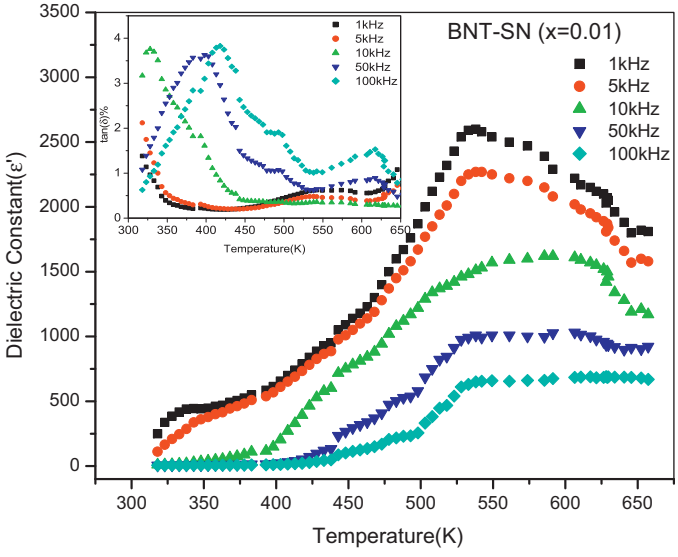

Fig. 2. Temperature dependence of dielectric constant of BNT–SN. Inset shows the temperature dependence of tangent loss.

Table 1
Curie temperature T_c and dielectric constant values at different frequencies in BNT–SN.

Frequency (kHz)	T_c (K)	ε'_m
1	538	2270
5	548	1780
10	556	1620
50	565	997
100	585	684

values of dielectric constant (ε') increase with increase in temperature and a peak evolves at 538 K (ε_m = 2250). Dielectric permittivity ε' shows a broad maximum at ferro–paraelectric phase transition temperature (T_c); the maximum value of ε' (ε_{max}) decreases with increase in frequency. The dielectric response of lead free relaxor BNT–SN, which indicates typical frequency dispersion (47 K), shift in dielectric maxima temperature (T_m) toward higher temperature side with increase in frequency (shown in Table 1), matched well with the earlier reports [32].

The diffused and frequency dispersive maximum in the temperature dependent relative permittivity (ε'), indicates that the dielectric polarization has a relaxation type behavior and the material is relaxor. The dielectric losses ($\tan\delta$, %) at different frequencies are shown in the inset of the Fig. 2. The tangent loss of BNT–SN shows higher values at lower temperature. It can be explained by well known macro-domain to micro-domain transition theory [33]. The dielectric loss in BNT-based ferroelectrics ceramics arises from the domain walls, and with the increasing temperature, macro-domains shift to micro-domain and the domain walls sharply increases, which leads to increase of dielectric loss at lower temperature. Further, increase in temperature micro-domains change to polar micro-regions and domain-walls decreases and hence decrease in dielectric loss which leads to a distinguished peak in dielectric loss–temperature curve corresponding to T_f.

Fig. 3 shows the inverse dielectric constant as a function of temperature performed at 1 kHz. A deviation from the Curie–Weiss law can be observed (Fig. 3). This deviation is a typical behavior of ferroelectric materials with diffuse phase transition. The parameter ΔT_m describes the degree of deviation from the Curie–Weiss law and is defined as $\Delta T_m = T_{cw} - T_m$, where T_{cw} denotes the temperature where the dielectric permittivity starts to deviate from the Curie–Weiss law and T_m is the temperature of the dielectric maximum [34]. The obtained results are presented in Table 2. In the

Table 2
Characteristic parameters determined and calculated from temperature dependence dielectric constant $\varepsilon'(T)$ measurements.

Frequency (kHz)	T_m (K)	Θ (K)	T_{cw} (K)	$\Delta T_m = T_{cw} - T_m$
1	538	580	608	70

temperature range between T_m and T_{cw}, modified Curie law is used to explain the dielectric behavior of complex ferroelectrics with diffuse phase transition, described as [35].

$$\frac{1}{\varepsilon'} - \frac{1}{\varepsilon'_m} = \frac{(T - T_m)^\gamma}{C'} \quad (1)$$

where γ and C' are measured to be constants, the value of γ lies between 1 and 2. The parameter γ gives information on the phase transition character; $\gamma = 1$ represents classical ferroelectric phase transition where normal Curie–Weiss law is followed and $\gamma = 2$ gives the quadratic dependence which describes complete diffuse phase transition. Fig. 4 shows the plot of $\log(1/\varepsilon - 1/\varepsilon_m)$ as a function of $\log(T - T_m)$ at 1 kHz. A linear relationship is obvious from the plot. The value of γ estimated from the slope of the graph is 1.82, indicating that the material has almost complete diffuse phase transition characteristics. For a more detailed insight into the relaxation process in the relative dielectric permittivity, a graph of $10^3/T_m$ was plotted as a function of $\log(\nu)$, as shown in Fig. 5. The nonlinear nature indicates that the data cannot be fitted by the simple Debye equation. In order to analyze the relaxation characteristics of BNT–SN ceramic, the experimental curves were fitted using the Vogel–Fulcher equation [36,37]:

$$\nu = \nu_0 \exp\left[\frac{-E_a}{k_B(T_m - T_f)}\right] \quad (2)$$

where ν_0 is the attempt frequency, E_a is the measure of average activation energy, k_B is the Boltzmann constant and T_f is the freezing temperature. The fitting parameters are T_f = 412.4 K, E_a = 0.053 eV and $\nu_0 = 1.6 \times 10^{13}$ Hz. Another parameter $\Delta T_{m\,(relax)}$ is used to characterize the degree of relaxation behavior in the frequency range of 1 kHz to 100 kHz, described [38] as

$$\Delta T_{m\ (relax)} = T_{m\ (100\,kHz)} - T_{m\ (1\,kHz)} \quad (3)$$

$\Delta T_{m\,(relax)}$, obtained from the dielectric measurements (Table 1) is approximately 47 K.

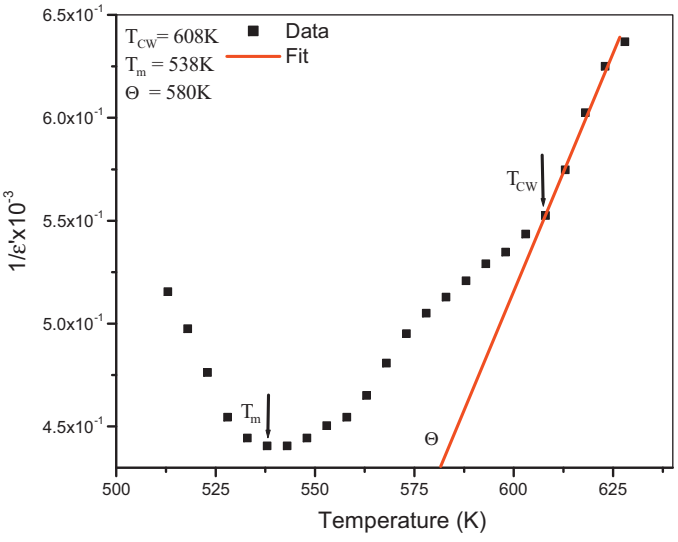

Fig. 3. Temperature dependence of the reciprocal dielectric constant ($1/\varepsilon'$) for BNT–SN fitted with Curie–Weiss law at 1 kHz.

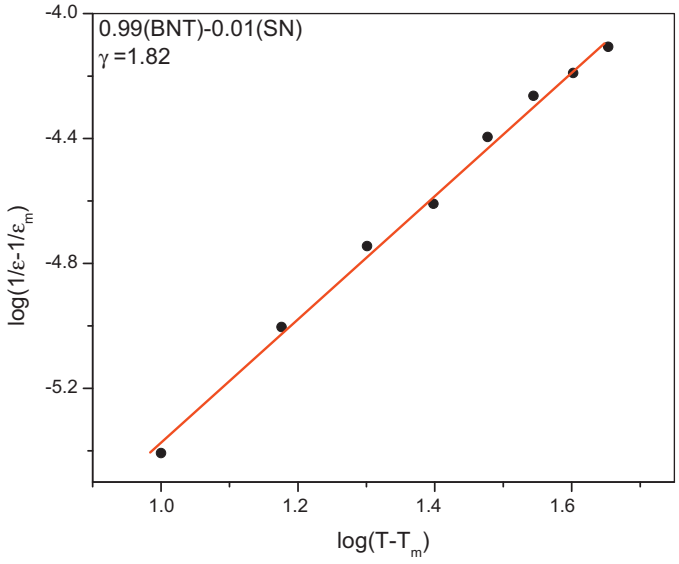

Fig. 4. $\log(1/\varepsilon - 1/\varepsilon_m)$ as a function of $\log(T - T_m)$ for BNT–SN at 1 kHz.

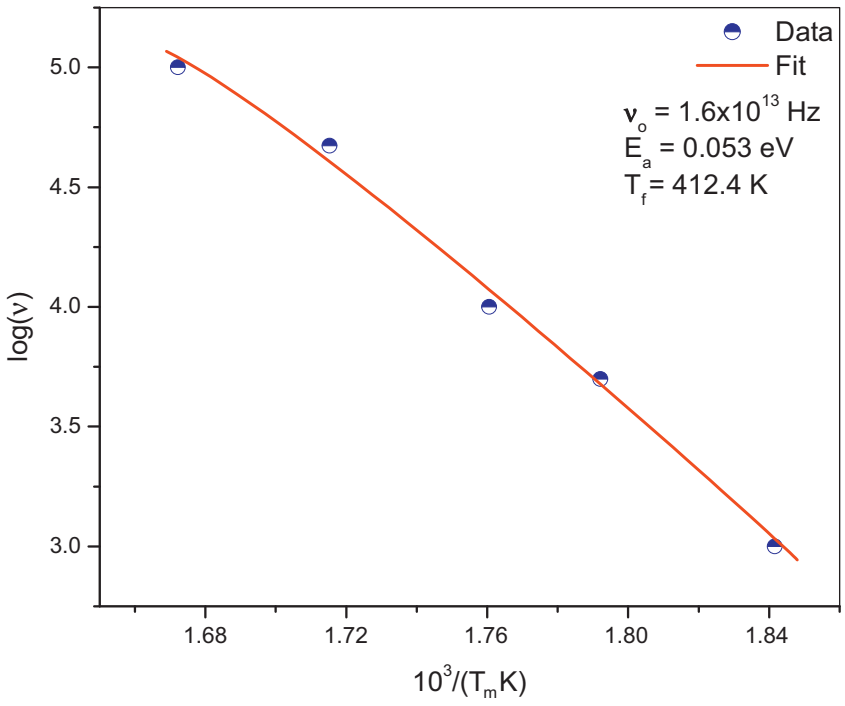

Fig. 5. log(ω) versus l/T_m plot. The solid line represents the fitting to Vogel–Fulcher relationship.

Frequency dependence of dielectric constant and corresponding loss are shown in Figs. 6 and 7 respectively. A general feature of the dielectric response is that dielectric constant values decrease with increasing the frequency of excitation and the high frequency dielectric behavior becomes temperature independent. Dielectric loss shows peak, which varies with temperature. The value of (ε') at lower frequencies in general, increases with decreasing frequency and increasing temperature. This may be attributed to be free charge buildup at the interface between the sample and the electrode (space charge polarization).

For a given temperature, the magnitude of ε' decreases with increasing frequencies, which is a typical characteristic of disordered materials [39,40]. The Debye formula giving complex permittivity related to free dipole oscillating in an alternating field [41] is given as:

$$\varepsilon^* = \varepsilon' - j\varepsilon'' = \varepsilon_\infty + \frac{\varepsilon_s - \varepsilon_\infty}{1 + j\omega\tau} \quad (4)$$

where ε_s and ε_∞ are the low and high frequency value of $\varepsilon'(\omega)$, $\omega = 2\pi\nu$, ν being the measuring frequency, τ is the relaxation time. Theoretical fitting of dielectric data (dielectric constant and dielectric loss) using Eq. (4) is shown in Figs. 6 and 7, for BNT–SN, it is clear that the experimental behavior follow the Debye equation. However, the contribution for dielectric constant is overestimated by the Debye equation especially at lower frequencies and the experimentally observed loss peaks are more diffused than those expected from single relaxation process of Debye. Deviation from the Debye behavior is a clear indication of system becoming more diffuse and disorder in the material. Obviously, one expects the

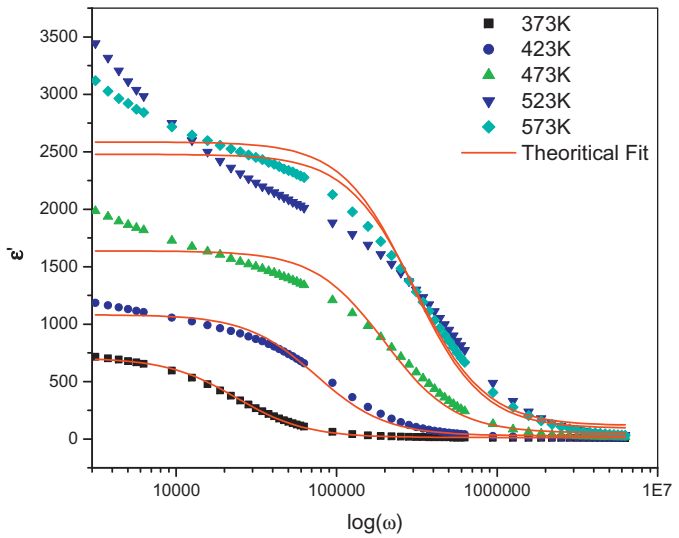

Fig. 6. Theoretical curve fit of frequency dependence of ε' for BNT–SN at various temperatures using the Debye formalism. Solid curves are theoretical fits.

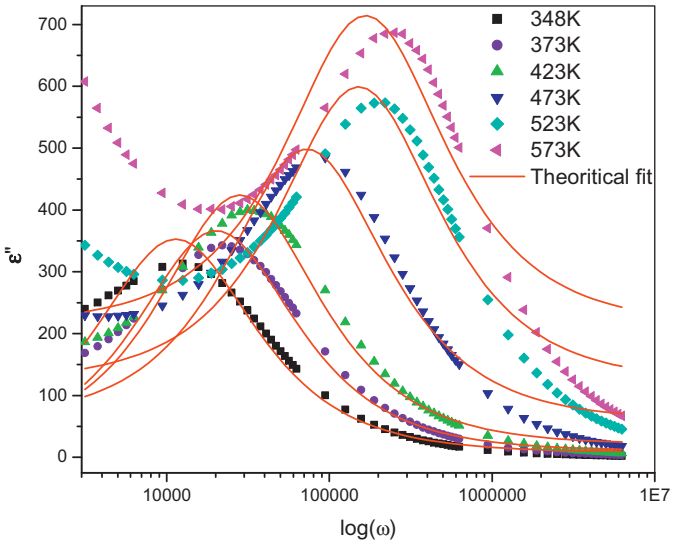

Fig. 7. Theoretical curves fit of frequency dependence of tan δ for BNT–SN at various temperatures using the Debye formalism. Solid curves are theoretical fits.

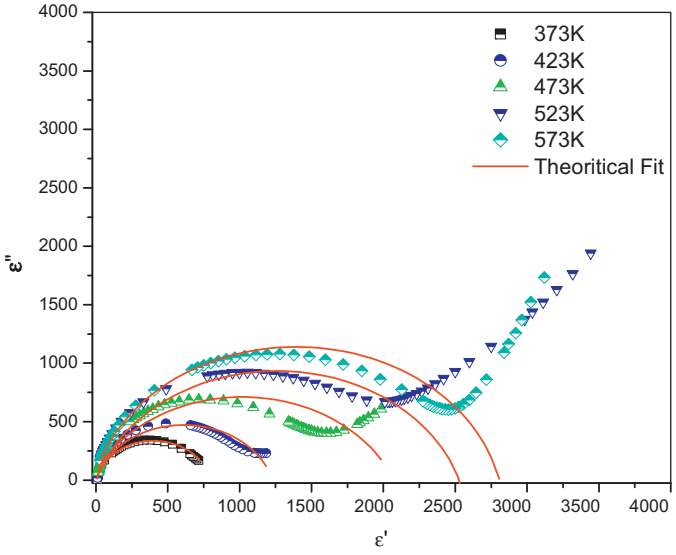

Fig. 8. Cole–Cole plots between ε' and ε'' for BNT–SN at some representative temperatures. Solid curves are theoretical fits.

Table 3
Static relative permittivity ε_s, optical relative permittivity ε_∞, global average relaxation time τ and tilt parameter α obtained from the Cole–Cole expression for BNT–SN.

Temperature (K)	ε_s	ε_∞	τ	α
373	705.29	12.70	1.0×10^{-6}	0.17
423	1081.48	28.08	3.2×10^{-6}	0.20
473	1637.40	52.66	5.3×10^{-6}	0.23
523	2477.82	89.71	6.2×10^{-6}	0.24
573	2585.25	91.6291	9.3×10^{-6}	0.26

poly-dispersive nature of relaxation processes. In order to understand the diffusion processes operating the system, the Cole–Cole formalism is adopted for analyzing the frequency dependence of dielectric response. The Debye equation (4) is modified in order to introduce diffuseness parameter as [42]

$$\varepsilon^* = \varepsilon' - j\varepsilon'' = \varepsilon_\infty + \frac{\varepsilon_s - \varepsilon_\infty}{(1 + j\omega\tau)^{1-\alpha}} \quad (5)$$

where ε_s and ε_∞ are the low and high frequency values of ε', α is a measure of the distribution of relaxation times, $\tau = \omega^{-1}$. The parameter, α can be determined from the location of the center of the Cole–Cole circles, of which only an arc lies above the ε' axis. Such plots are shown in Fig. 8. It is evident from these plots that the relaxation process differs from the Debye process (for which $\alpha = 0$). The parameter, α as determined from the angle subtended by the radius of the circle with the real axis passing through the origin of ε'-axis, shows a consistent increase in the interval (0.17–0.26) with increasing temperature from 373 K to 573 K. This means that relaxation time distribution decreases with decrease in temperature. Thus the Cole–Cole plots indicate the polydispersive nature of the dielectric relaxation in BNT–SN. Static relative permittivity ε_s, optical relative permittivity ε_∞ global average relaxation time τ and tilt parameter α obtained from the Cole–Cole expression for BNT–SN are given in Table 3.

4. Conclusions

$0.99(Bi_{0.5}Na_{0.5}TiO_3)$–$0.01(SrNb_2O_6)$ (BNT–SN) was prepared by simple solid state reaction route. Material stabilized in rhombohedral perovskite phase with lattice constants obtained for BNT–SN is $a = 3.9060$ Å, $\alpha = 89.86^\circ$ and $a_h = 5.4852$ Å, $c_h = 6.7335$ Å for hexagonal unit cells. The values of dielectric constant increase with increase in temperature and a peak evolves at 538 K ($\varepsilon_m = 2270$) at 1 kHz. Modified Curie law, indicates that the material has almost complete diffuse phase transition characteristics with $\gamma = 1.82$. The reciprocal dielectric constant $(1/\varepsilon')$ at 1 kHz fitted to the Curie–Weiss law and calculate the parameters $T_m = 538$ K, $T_{cw} = 608$ K and the difference between two temperatures, $\Delta T_m = T_{cw} - T_m$ (70 K) used as a characteristic diffuseness of phase transition. Vogel–Fulcher law fitting parameters are found as pre-exponential factor ω_o (1.6×10^{13} Hz), activation energy E_a (0.053 eV) and freezing temperature T_f (412.4 K). The low frequency dielectric dispersion is observed in BNT–SN. Cole–Cole plots of dielectric constant indicate polydispersive nature of the dielectric relaxation.

References

[1] Y. Yamashita, Jpn. J. Appl. Phys. 33 (1994) 4652.
[2] F. Yuan, Z. Peng, J.-M. Liu, Mater. Sci. Eng. B117 (2005) 265.
[3] G.A. Smolenski, V.A. Isupov, A.I. Aganovskaya, J. Sov. Phys. Solid State 2 (1961) 2651.
[4] T. Takenaka, H. Nagata, J. Eur. Ceram. Soc. 25 (12) (2005) 2693.
[5] C.R. Zhou, X.Y. Liu, W.Z. Li, C.L. Yuan, Solid State Commun. 149 (2009) 481.
[6] N. Jaitanong, W.C. Vittayakorn, A. Chaipanich, Ceram. Int. 36 (2010) 1479.
[7] K. Yoshii, Y. Hiruma, H. Nagata, T. Takenaka, Jpn. J. Appl. Phys. 45 (2006) 4493.
[8] Z. Yang, Y. Hou, H. Pan, Y. Chang, J. Alloys Compd. 480 (2009) 246.
[9] Y.M. Li, W. Chen, J. Zhou, Q. Xu, H.J. Sun, R.X. Xu, Mater. Sci. Eng. B 112 (2004) 5.
[10] D. Lin, D. Xiao, J. Zhu, P. Yu, J. Eur. Ceram. Soc. 26 (2006) 3247.
[11] D. Lin, K.W. Kwok, H.L.W. Chan, J. Alloys Compd. 481 (2009) 310.
[12] J. Shieh, K.C. Wu, C.S. Chen, Acta Mater. 55 (2007) 3081.
[13] D. Lin, C. Xu, Q. Zheng, Y. Wei, D. Gao, J. Mater. Sci. Mater. Electron. 20 (2009) 393.
[14] C. Xu, D. Lin, K.W. Kwok, Solid State Sci. 10 (2008) 934.
[15] L.W. David, A.P. David, J. Am. Ceram. Soc. 86 (2003) 769.
[16] J. Richard, G. Pettry, S. Said, P. Marchet, J.P. Mercurio, J. Eur. Ceram. Soc. 24 (2004) 1165.
[17] K.S. Rao, K.C.V. Rajulu, B. Tilak, A. Swathi, Nat. Sci. 2 (4) (2010) 357.
[18] J. Shi, W. Yang, J. Alloys Compd. 472 (2009) 267.
[19] M.V.M. Rao, C.-F. Kao, Physics B 403 (2008) 3596.
[20] C. Zhou, X. Liu, W. Li, C. Yuan, Mater. Res. Bull. 44 (2009) 724.
[21] P. Fu, Z. Xu, R. Chu, W. Li, G. Zang, J. Hao, Mater. Des. 31 (2010) 796.
[22] Changrong Zhou, Xinyu Liu, Weizhou Li, Changlai Yuan, J. Mater. Sci. Mater. Electron. 21 (2010) 364.
[23] CerneaF M., AndronescuF E., RaduF R., F. Fochi, C. Galassi, J. Alloys Compd. 490 (2010) 690.
[24] C.-R. Zhou, X.-Y. Liu, Bull. Mater. Sci. 30 (2007) 575.
[25] E. Wu, "POWD", An Interactive Powder Diffraction Data Interpretation and Indexing Programme, Ver. 2.1, School of Physical Sciences, Flinders University of South Australia, Bedford Park, S.A. 5042, Australia.
[26] C. Peng, J.-F. Li, W. Gong, Mater. Lett. 59 (2005) 1576.
[27] A. Rachakom, S. Jiansirisomboon, A. Watcharapasorn, J. Microsc. Soc. Thailand 23 (2009) 107.
[28] Y. Liu, Y. Lv, M. Xu., S. Shi, H. Xu, X. Yang, J. Wuhan Univ. Technol. Mater. Sci. Ed. (June 2007).
[29] Q. Yangfang, S. Dan, S. Jianjing, Mater. Sci. Eng. B121 (2005) 148.
[30] Y.M. Li, W. Chen, J. Zhou, Mater. Sci. Eng. B112 (2004) 5.
[31] S. Said, J. Mercurio, J. Eur. Ceram. Soc. 21 (2001) 1333.
[32] I. Rivera, Ashok Kumar, N. Ortega, KatiyarF R.S., Sergey Lushnikov Solid State Commun. 149 (2009) 172.
[33] X. Yao, Z.L. Chen, L.E. Cross, J. Appl. Phys. 54 (1983) 3394.
[34] X.G. Tang, X.X. Wang, K.-H. Chew, H.L.W. Chan, Solid State Commun. 136 (2005) 89.
[35] G. Fulcher, J. Am. Ceram. Soc. 8 (1925) 339.
[36] Y. Guo, K. Kakimoto, H. Ohsato, J. Phys. Chem. Solids 65 (2004) 1831.
[37] S.K. Rout, T. Badapanda, E. Sinha, S. Panigrahi, P.K. Barhai, T.P. Sinha, Appl. Phys. A 91 (2008) 101.
[38] C. Ang, Z. Jing, Z. Yu, J. Phys. Condens. Matter 14 (2002) 8901.
[39] M. Pastor, P.K. Bajpai, R.N Chaudhury, Physics B 391 (2007) 1.
[40] M. Pastor, P.K. Bajpai, R.N Chaudhury, Bull. Mater. Sci. 28 (2005) 199.
[41] A. Chelkowski, Dielectric Physics, in: Studies in Physical and Theoretical Chemistry, vol. 9, Elsevier Scientific Pub. Co., Amsterdam, 1980, p. 119.
[42] K.S. Cole, R.H. Cole, J. Chem. Phys. 9 (1941) 341.